

Electrochemical performance and redox stability of $\text{Sr}_{0.8}\text{La}_{0.2}\text{TiO}_3\text{-Ce}_{0.9}\text{Gd}_{0.1}\text{O}_{2-\delta}$ composite anodes for solid oxide fuel cells

Manasa K. Rath^a, Ji-Hoon Koo^a and Ki-Tae Lee^{a,b,*}

^aDivision of Advanced Materials Engineering

^bHydrogen and Fuel Cell Research Center, Chonbuk National University, Jeonbuk 54896, Korea

$\text{Sr}_{0.8}\text{La}_{0.2}\text{TiO}_3\text{-Ce}_{0.9}\text{Gd}_{0.1}\text{O}_{2-\delta}$ (SLT-GDC) composite anodes were synthesized by solid state reaction and the effect of percolation on electro-catalytic activity and redox stability was investigated. The percolation threshold of $\text{Sr}_{0.8}\text{La}_{0.2}\text{TiO}_3$ and $\text{Ce}_{0.9}\text{Gd}_{0.1}\text{O}_{2-\delta}$ in the composite calculated based on the Kusy's percolation theory is 10.7 vol.% and 17.4 vol.%, respectively. The area specific resistance (ASR) of the SLT-GDC composite anode at 800 °C in H_2 decreased up to 15 vol.% GDC in a SLT matrix because GDC has a much higher electro-catalytic activity than SLT. However, the samples which showed GDC percolation, including samples with 20 and 33 vol.% GDC in a SLT matrix, showed very high ASR values. The lowest ASR value was obtained for the anode with 15 vol.% GDC in a SLT matrix because this anode showed a mixed percolation region and had good connectivity to both electronic and ionic compounds. Moreover, the anode with the 15 vol.% GDC in a SLT matrix has very stable activity with a deviation of only 0.5% in ASR during repeated redox cycling.

Key words: Solid oxide fuel cell, Composite anode, Percolation, Redox stability.

Introduction

Solid oxide fuel cells (SOFCs) are energy conversion devices that convert chemical fuels directly into electricity by an electrochemical combustion reaction of fuel and oxygen. In SOFCs, the anode is operated under highly reducing conditions [1-2]. Therefore, the development of highly active and redox stable anode materials is crucial to achieving successful commercialization. Ni-based cermet anodes are state-of-the-art anode materials for SOFCs. These materials show high catalytic activity, electrical conductivity, and excellent electro-chemical performance under H_2 fuel. However, there are some problems related to Ni-cermet anodes such as Ni-coarsening during long term operation, poor redox stability, and carbon coking and deactivation when using hydrocarbon fuel.

Perovskite-based catalysts such as LaCrO_3 and SrTiO_3 are alternative electro-ceramics that can be used to overcome the above issues [3]. Rare earth doped SrTiO_3 based perovskite has shown particularly high electrical conductivity and redox stability under a wide range of oxygen partial pressures and anode operating conditions [4]. However, La doped SrTiO_3 (SLT) has shown lower activity for H_2 oxidation compared to Ni-cermet anodes. To improve its electro-catalytic performance, SLT has been combined with other ionic conductors or active catalysts to form a composite [5-8]. In this study, we

investigated the percolation effect on the electrochemical properties and redox stability of $\text{Sr}_{0.8}\text{La}_{0.2}\text{TiO}_3$ (SLT)-GDC ($\text{Ce}_{0.9}\text{Gd}_{0.1}\text{O}_{2-\delta}$) composite anodes.

Experimental

$\text{Sr}_{0.8}\text{La}_{0.2}\text{TiO}_3$ (SLT) powder was synthesized using LaO_3 , SrCO_3 , and TiO_2 (Alfa Aesar, 99.9%) as precursor materials by a conventional solid-state reaction. Stoichiometric amounts of the precursors were mixed by ball-milling for 12 hrs followed by calcination at 1100°C for 3 hrs in air. To make SLT-GDC composites, the calculated amount of commercial GDC (CGO90/10 UHSA, Grand C&M Co. Ltd.) powder was mixed with the synthesized SLT powder by a ball milling process. SLT-GDC composite powders with various amounts of GDC were prepared. For convenience, we refer to pure SLT as “SG0”, while “SGx” refers to GDC in a SLT matrix where x represents the vol.% of GDC (i.e., x = 10, 15, 20 and 33).

Electrochemical performance was evaluated using symmetric half-cells. The symmetric half-cells had a geometrical electrode area of 0.25 cm² and were fabricated using a screen-printing method. The electrode paste was prepared by mixing the powder and binder (Heraeus V006) at a ratio of 70 : 30 wt.% for 30 minutes with a paste mixer machine (PDM-300 Daehwa Tech., Korea). Then, the paste was screen-printed on both sides of a $\text{La}_{0.8}\text{Sr}_{0.2}\text{Ga}_{0.8}\text{Mg}_{0.2}\text{O}_3$ (LSGM) disk. The screen-printed layers were then fired at 1300 °C for 2 hrs. AC impedance analysis for the symmetric half-cells was carried out using a galvanopotentiostat (SP150, Biologic

*Corresponding author:
Tel : +82-63-270-2290
Fax: +82-63-270-2386
E-mail: ktlee71@jbnu.ac.kr

SAS, France) with a frequency response analyzer under open-circuit conditions at 800 °C. The applied frequency was in the range of 0.1 mHz to 1 MHz with a voltage amplitude of 25 mV. Humidified (3% H₂O) H₂ fuel was fed at a rate of 100 cm³ min⁻¹.

Results and Discussion

The crystalline phase and the chemical stability of the composites were determined by X-ray diffraction (XRD, D/MAX-111A Rigaku, Japan), which employed Cu K α radiation. XRD patterns of the pure Sr_{0.8}La_{0.2}TiO₃ calcined at 1100 °C for 3 hrs in air and SLT-GDC composites fired at 1400 °C for 10 hrs in air are shown in Fig. 1. All peaks in the XRD patterns correspond to either Sr_{0.8}La_{0.2}TiO₃ (JCPDS #01-079-0181) or Ce_{0.9}Gd_{0.1}O_{1.95} (JCPDS #75-0161). No trace of secondary peaks in the XRD patterns was observed. This indicates that the composites are thermally stable and that there was no interfacial reaction between SLT and GDC even at high temperature.

Particle sizes of SLT and GDC were 2.1 and 0.3 μ m, respectively, as measured using dynamic light scattering. The percolation threshold volume was calculated using Kusy's percolation theory given as [9]:

$$V_c = \frac{100}{1 + \left(\frac{\phi}{4x_c}\right)\left(\frac{R_p}{R_m}\right)} \quad (1)$$

Here, V_c is the percentage of dispersed volume in the SLT-GDC matrix, R_p is the radius of the primary phase particle (SLT), and R_m is radius of the dispersed phase particle (GDC). We assumed that the GDC particles were packed in a cubic manner in the composite matrix, and, for cubic packing, $\Phi = 1.27$ and $X_c = 0.42$. Based on Kusy's percolation theory, the calculated percolation volume of GDC in the SLT matrix is 17.4 vol.%, and that of SLT in the GDC matrix is 10.7 vol.%.

The microstructure of the composite catalyst plays an

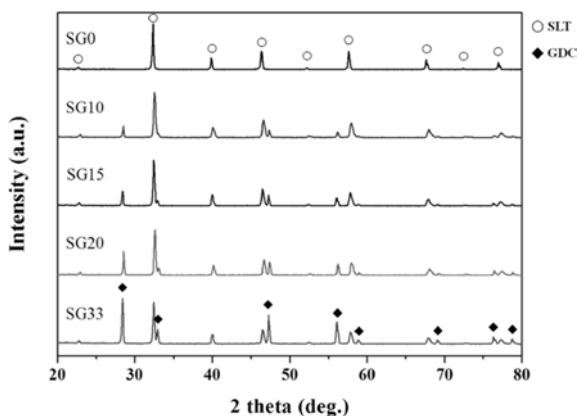


Fig. 1. X-ray diffraction patterns of pure SLT calcined at 1100 °C for 3 hrs in air and SLT-GDC composites fired at 1400 °C for 10 hrs in air.

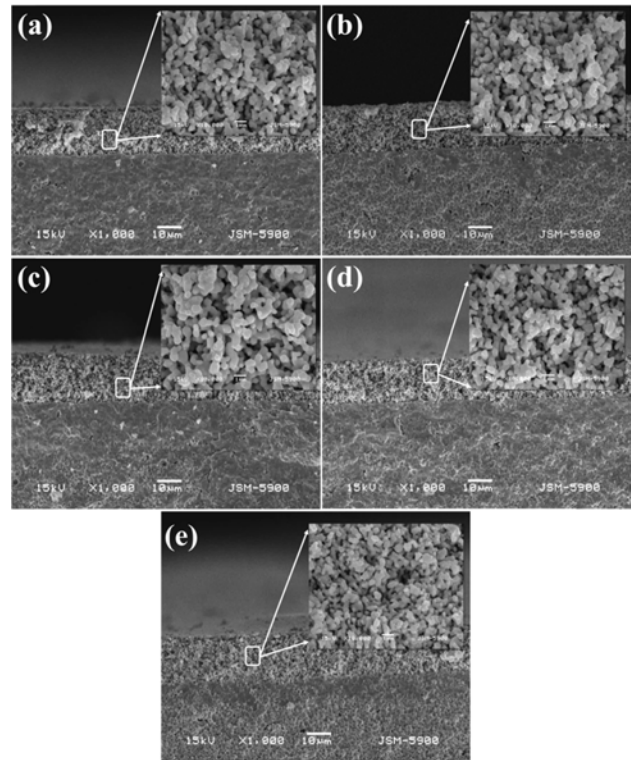


Fig. 2. Cross-sectional SEM micrographs of (a) SG0, (b) SG10, (c) SG15, (d) SG20, and (e) SG33 on LSGM electrolytes. The inset shows an enlarged micrograph of the selected anode region.

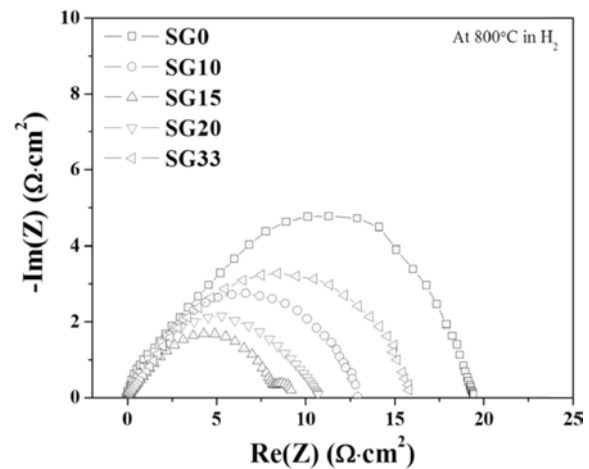


Fig. 3. AC impedance spectra of pure SLT and SLT-GDC composites under humidified H₂ at 800 °C.

important role in the catalytic oxidation of H₂ [10]. Cross-sectional images of the LSGM|SG_x symmetric half-cells sintered at 1300 °C are given in Fig. 2. All the anodes were composed of the catalysts and homogeneously distributed micro-pores. As shown in Fig. 2, there was an area contact between the particles and good adhesion between the anode and electrolyte. Moreover, all the anodes have similar thicknesses of ~20 μ m and similar morphology and porosity.

Nyquist plots for H₂ oxidation of the SLT and SG_x composites at 800 °C are given in Fig. 3. The polarization

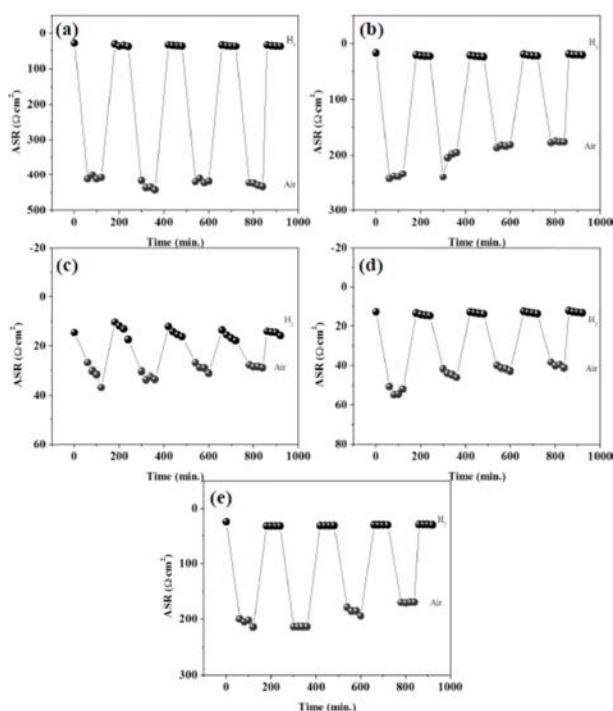


Fig. 4. Area specific resistance of (a) SG0, (b) SG10, (c) SG15, (d) SG20, and (e) SG33 anodes measured under cyclic reduction and oxidation at 800 °C.

resistance value decreases up to $x = 15$ and then increases significantly with increasing GDC content. We expected that the polarization resistance of the SLT-GDC composite would decrease with increasing GDC content because GDC has a much higher electro-catalytic activity than SLT. On the other hand, GDC has a significantly lower electrical conductivity than SLT. Therefore, the samples within the GDC percolation region (such as SG20 and SG33) showed high polarization resistance values caused by slow charge transfer reactions and low electrical conductivity. Previous work has shown that incorporation of doped ceria into an electro-ceramic catalyst improved the catalytic activity; this improvement was attributed to an optimized electrical conduction path, which established a connection to the catalytic reaction zones during H_2 oxidation [11, 12].

Redox-stability tests for cyclic reduction and oxidation were performed by flowing H_2 followed by purging with N_2 gas for 20 minutes, and then introducing air into the cell at 800 °C. Impedance data were recorded after each reduction and oxidation step over 5 cycles. The polarization resistance of all the anodes during each

reduction and oxidation are plotted in Fig. 4. Area specific resistance (ASR) values in H_2 were 27.5, 16.9, 12.4, 14.7, and 23.4 $\Omega\text{ cm}^2$ for SG0, SG10, SG15, SG20, and SG33, respectively. However, the ASR value of each anode increased significantly during oxidation. Our results demonstrate that the SG15 anode has very stable activity with a deviation of only 0.5% in ASR during repeated redox cycling.

Conclusions

In order to make optimized SLT-GDC composite anodes, Kusy's percolation theory was adopted to determine the desired composite composition. The electro-catalytic activity of SLT-GDC composites changed based on SLT and GDC content. The polarization resistance of SLT-GDC composites decreased with increasing GDC content in the SLT percolation region and then increased in the GDC percolation region. The sample with 15 vol.% GDC (SG15) showed the least polarization resistance and best stability during complete redox cycling because it operates in the mixed percolation region and has optimal connectivity between electronic and ionic compounds.

Acknowledgements

This paper was supported by research funds of Chonbuk National University in 2015.

References

1. N.Q. Minh, *J. Am. Ceram. Soc.* 76 (1993) 563.
2. S.C. Singhal, *Solid State Ionics* 135 (2000) 305.
3. S.W. Tao, J.T.S. Irvine, *Nat. Mater.* 2 (2003) 320.
4. X. Li, H. Zhao, W. Shen, F. Gao, X. Huang, Y. Li, Z. Zhu, *J. Power Sources* 166 (2007) 47.
5. M.D. Gross, J.M. Vohs, R.J. Gorte, *Electrochem. Solid-State Lett.* 10 (2007) B65.
6. G. Kim, M.D. Gross, W. Wang, J.M. Vohs, R.J. Gorte, *J. Electrochem. Soc.* 155 (2008) B360.
7. S. Lee, G. Kim, J.M. Vohs, R.J. Gorte, *J. Electrochem. Soc.* 155 (2008) B1179.
8. M.A. Buccheri, J.M. Hill, *J. Electrochem. Soc.* 159 (2012) B361.
9. R.P. Kusy, *J. Appl. Phys.* 48 (1977) 5301.
10. P.S. Jørgensen, S.L. Ebbenhøj, A. Hauch, *J. Power Sources* 279 (2015) 686.
11. K.B. Yoo, B.H. Park, G.M. Choi, *Solid State Ionics* 225 (2012) 104.
12. M.K. Rath, B.H. Choi, K.T. Lee, *J. Power Sources* 213 (2012) 55.